

Design Study and Analysis of Hybrid Excitation Flux Switching Motor with DC Excitation in Radial Direction

E. Sulaiman¹, N. S. M. Amin¹, Z. A. Husin¹, M. Z. Ahmad¹ and T. Kosaka²

¹Universiti Tun Hussein Onn Malaysia, Locked Bag 101, 86400 Malaysia

²Nagoya Institute of Technology, 466-8555, Nagoya, Japan

Abstract- Research and development of hybrid excitation flux switching motors (HEFSMs) that combined both permanent magnet (PM) and DC field excitation coil (FEC) as their main flux sources have been an attractive investigation recently due to their overwhelming performances as well as flux control capabilities. Among different types of HEFSMs, the motor with both PM and FEC located on the stator has the advantage of robust rotor structure due to their high mechanical stress suitable for high-speed applications. In this research, design and performance of a three-phase 12-slot 10-pole HEFSM in which the DC FEC in radial direction on the stator are investigated. Initially, coil arrangement test is analyzed to all armature coil slots to confirm the polarity of the phase. Then, flux interaction analysis is performed to investigate the flux capabilities at various current densities. Finally, torque and power performances are investigated at various armature and FEC current densities. The results show that the proposed motor has proportional increment of torque and power with respect with the current density suitable for various applications.

I. INTRODUCTION

With dramatic accomplishments and developments of power electronics devices and permanent magnet (PM) materials, brushless machines stimulated by PM and DC FEC flux are developing significantly for various applications. As the PM flux is always constant, the DC FEC provides variable flux control capabilities in term of field strengthening or field weakening circumstances. These machines are called hybrid excitation machines (HEMs) which generally categorized into four groups. The first type consists of both PM and DC FEC embedded in rotor part while the armature coil is placed in stator body, such as combination rotor hybrid excitation machines (CRHEMs) and PM hybrid synchronous machines [1-3]. The second type consists of PM in the rotor while DC FEC in the stator [4], whilst the third type consists of PM in the rotor and DC FEC in the machine end [5-6]. Finally, the fourth HEMs are the machine with both PM and DC FEC placed in the stator [7-9]. Among several HEMs, it should be highlighted that all HEMs mentioned in the first three are having a PM in rotor body and can be categorized as “hybrid rotor-PM with DC FEC machines” while the fourth machines can be referred as “hybrid stator-PM with DC FEC machines”. Based on its principles of operation, the fourth HEMs are also known as “hybrid excitation flux switching machines (HEFSMs)” which is getting more popular lately.

When compared with “hybrid rotor-PM with DC FEC machines” and conventional IPMSM [10], HEFSMs with all active parts, namely PM, DC FEC and armature coil located on the stator have advantages of robust rotor structure similar with switch reluctance machines (SRMs), suitable for high speed drive applications; simple cooling system for heat dissipation which makes it suitable to be applied in high current density condition, as well as variable flux capabilities from DC FEC.

II. HYBRID EXCITATION FLUX SWITCHING MACHINES

Hybrid excitation flux switching machines (HEFSMs) are those which utilize primary excitation by PMs as well as DC FEC as a secondary source. Conventionally, PMFSMs which employ PM flux only can be operated beyond base speed in the flux weakening region by means of controlling the armature winding current. By applying negative d-axis current, the PM flux can be counteracted. However it also suffers with several disadvantages of high copper loss, less power capability, less efficiency and also possible irreversible demagnetization of the PMs. Thus, HEFSM is an alternative option where the advantages of both PM machines and DC FEC synchronous machines are combined. As such HEFSMs have the potential to improve flux weakening performance, power and torque density, variable flux capability, and efficiency which have been researched extensively over many years [11-14].

Various combinations of stator slots and rotor poles for HEFSMs have been developed as illustrated in Fig. 1. Fig. 1(a) shows a 6-slot 4-pole HEFSM in which the active parts are arranged in three layers in the stator. The inner stator consists of the armature windings, followed by the DC FEC in the middle layer, while the PM is placed in outer stator [15-16]. However, the machine has low torque density and long end winding for the DC FEC, which overlaps the armature coil windings, and high copper loss.

Moreover, based on the topology of a purely PM excited PMFSM, a new 12-slot 10-pole HEFSM is developed [17], in which the PMs dimensions are reduced to save space for the introduced FEC windings, whilst both the stator and rotor laminations are unchanged as depicted in Fig. 1(b). It should be emphasized that the flux regulation capability of the machine can be simply controlled by adjusting the PM length

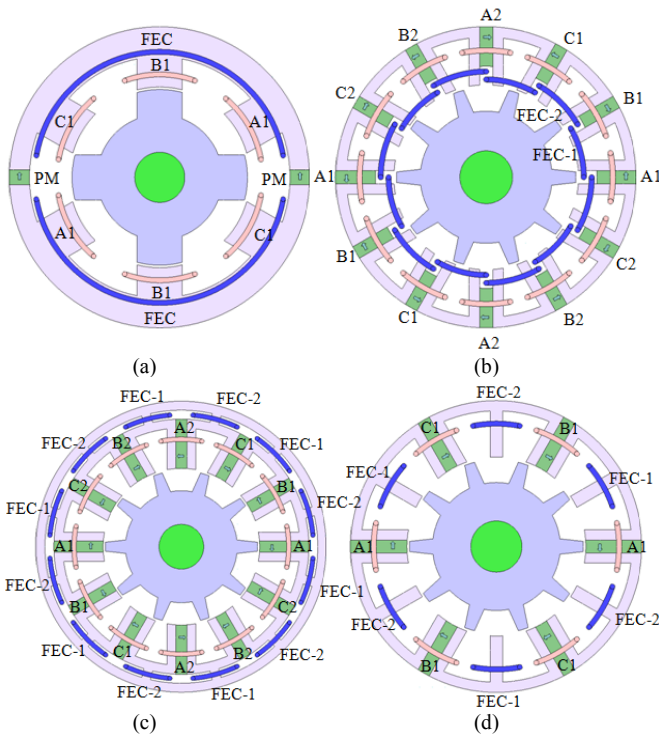


Fig. 1. Several HEFSMs topology (a) 6-slot 4-pole (b) 12-slot 10-pole with separated C-core stator (c) 12-slot 10-pole with DC FEC at outer stator (d) 6-slot 10-pole E-core HEFSM

in radial direction. Meanwhile, the HEFSM shown in Fig. 1(c) is a three-phase 12-slot 10-pole PMFSM which incorporates the DC FEC at outer extremity of the stator [18-19]. However, the outer diameter of the machine is significantly enlarged for the DC FEC winding, which in turn reduces torque density.

Besides, a new HEFSM is proposed by inserting DC FECs on the middle teeth of the E-core stator PMFSM, as shown in Fig. 1(d) [20]. It maintains the same outer diameter and exhibits a simpler 2-D structure than the HEFSM discussed in Fig. 1(c). In addition, it also yields non-overlap between DC FEC and armature windings. The number of turns per phase of the E-core HEFSM is maintained in which half of the slot area is employed for the armature windings, and another half is employed for the DC FECs.

However, the HEFSMs in Figs. 1(a), (b) and (d) have a PM along the radial of the stator, thus the flux of PM in the outer stator acts as a leakage flux and has no contribution towards the torque production which reduces the machine performance. In addition, due to segmented stator core, the final machine design is also difficult to manufacture. Whereas, the 12-slot 10-pole outer FEC HEFSM in Fig. 1(c) has no flux leakage outside the stator and it also has the single piece stator which is much easier to manufacture when compared with the other design of HEFSMs. Nevertheless, the original 12-slot 10-pole outer FEC HEFSM has a limitation of torque and power production in high current density condition due to insufficient stator yoke width between FEC and armature coil slots resulting in magnetic saturation and negative torque production. After some design modifications and

improvements especially on the stator yoke mentioned above including both armature coil and DC FEC slots area, the improved machine is able to operate at the target performances [21-23]. It should be noted that all HEFSM mentioned above are having an arrangement of armature coil and DC FEC in theta direction.

Based on several topology of HEFSM, a new 12-slot 10-pole HEFSM in which the arrangement of DC FEC in radial direction is proposed as depicted in Fig. 2. It is obvious that the main difference of the proposed HEFSM with other HEFSMs discussed above is the DC FEC configuration that are wound in radial polarity, when compared with theta polarity, respectively.

In this paper, design study and performance investigation of 12-slot 10-pole HEFSM with DC FEC in radial polarity are investigated. The design restrictions and specifications of the motor are discussed in Section III. The open circuit analysis such as armature coil test, PM flux distribution, cogging torque and flux linkage of PM with various DC FEC current density conditions analysis is examined in Section IV. In addition, the short circuit analysis such as flux interaction of PM, DC FEC and armature coil at maximum current density condition, instantaneous torque characteristic, and torque characteristics at various current density conditions are also predicted and discussed in Section V. Finally the conclusions are drawn in Section VI.

III. DESIGN RESTRICTION AND PARAMETER SPECIFICATIONS OF THE 12-SLOT 10-POLE HEFSM

The design restriction and parameter specifications of the proposed 12-slot 10-pole HEFSM are listed in Tables I and II, respectively. From Table I, the electrical restrictions related

TABLE I
HEFSM DESIGN RESTRICTIONS

| Electrical Restrictions | |
|--|-----|
| Max. DC-bus voltage inverter (V) | 650 |
| Max. inverter current (A_{rms}) | 240 |
| Max. armature coil current density, J_a (A_{rms}/mm^2) | 30 |
| Max. DC FEC current density, J_c (A/mm^2) | 30 |
| Geometrical Restrictions | |
| Stator outer diameter (mm) | 264 |
| Motor stack length (mm) | 70 |
| Shaft radius (mm) | 30 |
| Air gap length (mm) | 0.8 |
| PM weight (kg) | 1.0 |

TABLE II
HEFSM PARAMETER SPECIFICATIONS

| Parameter | Details | HEFSM |
|-----------|-------------------------------|-------|
| D_1 | Rotor radius (mm) | 84.2 |
| D_2 | Rotor pole height (mm) | 21.2 |
| D_3 | Rotor pole width (mm) | 10.0 |
| D_4 | PM height (mm) | 23.6 |
| D_5 | DC FEC width (mm) | 14.0 |
| D_6 | DC FEC height (mm) | 7.0 |
| D_7 | Armature coil width (mm) | 6.5 |
| D_8 | Armature coil height (mm) | 23.6 |
| N_a | No. of turns of armature coil | 7 |

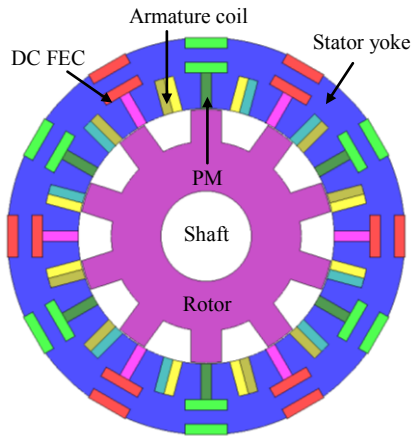


Fig. 2. Initial design of 12-slot 10-pole HEFSM with DC FEC in radial polarity

with the inverter such as maximum 650V DC bus voltage and maximum 240A inverter current are set. The limits of the current densities are set to the maximum of $30A_{rms}/mm^2$ and $30A/mm^2$ for armature winding and DC FEC, respectively. In addition, the geometrical dimensions of the HEFSM such as the stator outer diameter, motor stack length, shaft radius and air gap are set to 264mm, 70mm, 30mm and 0.8mm respectively, while the PM weight is set to be 1.0kg.

Meanwhile, the rotor parameters such as rotor radius, D_1 , rotor pole height, D_2 and pole width, D_3 are set to 84.2mm, 21.2mm and 10.0mm, respectively. Further, the PM height, D_4 is set to 23.6mm while the DC FEC weight and height, D_5 and D_6 are set to 14.0mm and 7.0mm, respectively. Finally, the armature coil width and height, D_7 and D_8 , are set to 6.5mm and 23.6mm, respectively, which gives the armature coil number of 7 turns.

Commercial FEA package, JMAG-Designer ver.12.0, released by Japanese Research Institute (JRI) is used as 2D-FEA solver for this design. The PM material used in for this motor is Neomax 35AH whose residual flux density and coercive force at $20C^\circ$ are 1.2T and 932kA/m, respectively while the electrical steel 35H210 is used for rotor and stator body.

IV. OPEN CIRCUIT TEST ANALYSIS

A. Armature Coil Arrangement Test of PM Flux

The arrangement of 12 armature coil is tested using coil test analysis to the design HEFSM as shown in Fig. 3. Initially, all armature coils are set in counter clockwise direction, while the PM and DC FEC polarities are set in alternate direction to create 12 north and 12 south poles respectively. Then, the flux linkage in each armature coil slot is analyzed for the motor running at speed of 1200r/min. At this condition, the flux source is mainly comes from the PM where the DC FEC current is set to 0A. From the analysis, it is found that four armature coil slots produce one phase of flux linkage, while the remaining eight armature coil slots also produce another two flux linkages with different phases. The three-phase flux linkage in which the flux source is produced by PM only is

illustrated in Fig. 4. From the graph, the flux characteristics can be considered as sinusoidal with maximum flux of approximately 0.0083Wb. Thus, it is expected that only small amount of induced voltage will be generated if the motor is to be applied in open circuit condition due to some failure which will not harm the motor.

B. PM Flux Distribution

The PM flux distribution of the 12-slot 10-pole HEFSM at zero rotor position is illustrated in Fig. 5. It is obvious that most of the PM flux flows from stator to rotor while the

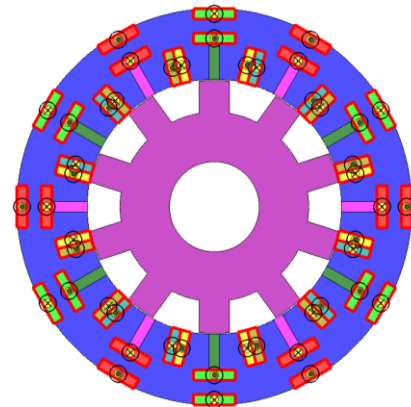


Fig. 3. Armature coil setting for coil test analysis

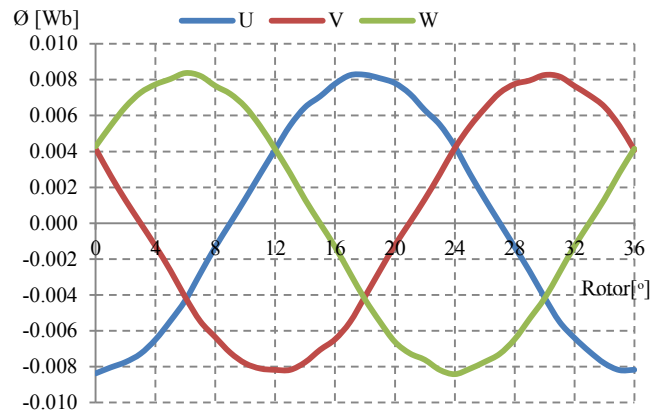


Fig. 4. Three-phase flux linkage produced by PM only

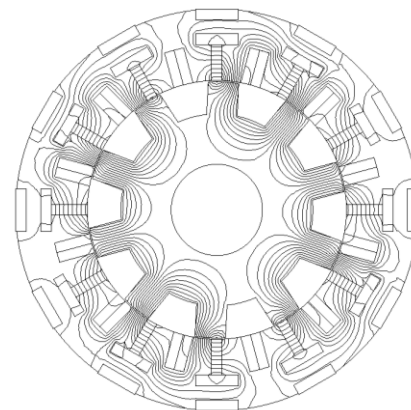


Fig. 5. PM flux distribution at zero rotor position

remaining flux flows around DC FEC pitch to form a complete of 12 cycle flux. However, huge number of flux flows in the rotor will results in high air gap flux density which lead to unnecessary flux leakage and flux cancellation. In addition, high flux density occurs between the armature coil and DC FEC slots which results in flux saturation.

C. PM Cogging Torque

Fig. 6 illustrates the PM cogging torque for one electric cycle of 36° rotor position. It is observed that the cogging torque generated is considered high with the maximum peak-to-peak of approximately 231Nm. This is due to the effect of high PM flux linkage flow to the rotor as discussed above. Thus, as one strategy that can reduce the cogging torque, design improvement by reducing stator width between armature coil and DC FEC to reduce the flux saturation can be conducted in future.

D. Flux Analysis of PM and DC FEC at Various Current Density Condition

The flux linkage of PM with various DC FEC current density conditions is illustrated in Fig. 7. It is obvious that similar flux shape is obtained with increasing DC FEC current density. At maximum DC FEC current density of $30\text{A}/\text{mm}^2$ the flux linkage increase more than four times when compared with flux linkage of PM only. The maximum flux linkage obtained at this condition is approximately 0.0435Wb. This condition proves that the additional DC FEC can improve the PM flux, thus giving variable flux control capability.

The analysis of maximum flux of PM with DC FEC and maximum DC FEC flux only, where the PM is set as air is depicted in Fig. 8. It is clear that the flux combination of PM with DC FEC produced much higher flux when compared with flux from DC FEC only. Besides, the DC FEC flux starts to decrease when higher DC FEC current density is injected to the system. This is due to higher flux generated at high current density can easily flows over the air slot of PM, thus keeping most of the flux in stator core. In contrast with flux of PM with DC FEC, the flux generated keep on increases with increasing DC FEC current density.

V. SHORT CIRCUIT TEST ANALYSIS

A. Flux Interaction Analysis of PM, DC FEC and Armature Coil at Maximum Current Density Condition

The flux generated from individual source of PM, DC FEC at $30\text{A}/\text{mm}^2$ and armature coil at maximum current density of $30\text{A}_{\text{rms}}/\text{mm}^2$ are compared and analyzed as shown in Fig. 9. When the PM is set to air, the generated flux is come either from DC FEC or armature coil only. The individual flux of PM, DC FEC and armature coil are highlighted in red, green and blue dotted line, respectively, while the resulting flux is illustrated in black line. The amplitude of PM flux, DC FEC flux at $30\text{A}/\text{mm}^2$, armature coil flux at $30\text{A}_{\text{rms}}/\text{mm}^2$, and resulting flux generated are 0.083Wb, 0.0133Wb, 0.0745Wb and 0.0764Wb, which give the torque and power of 94.35Nm and 11.86kW, respectively.

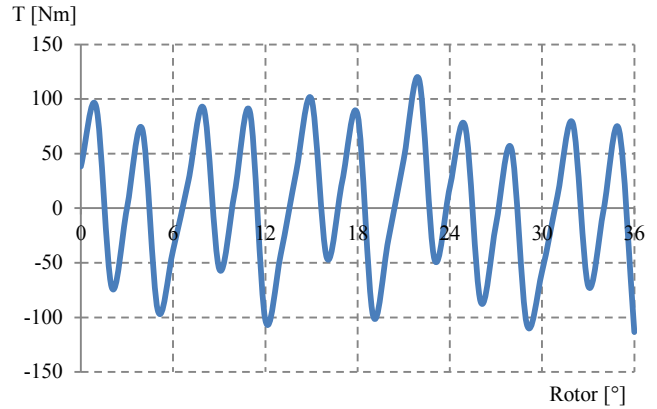


Fig.6. PM cogging torque

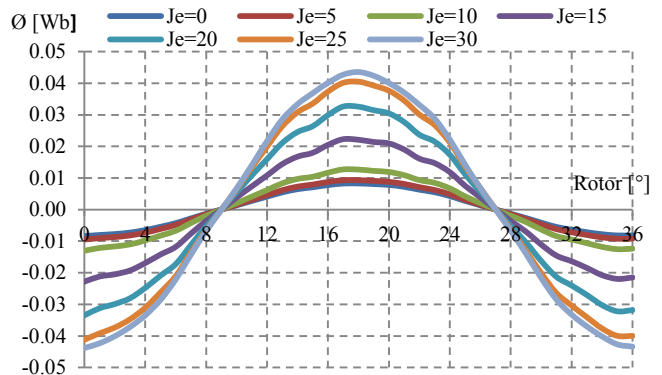


Fig.7. Flux linkage of PM with various DC FEC current densities, A/mm^2

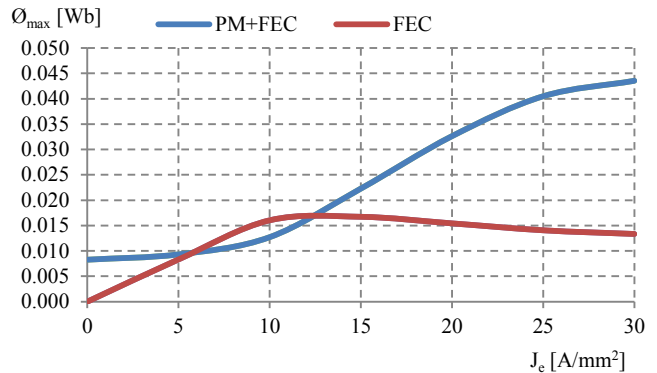


Fig.8. Comparison of maximum flux linkage of PM with DC FEC and flux from DC FEC only

B. Instantaneous Torque Characteristic at Maximum Current Density Condition

Fig. 10 illustrates the instantaneous torque waveform of the proposed HEFSM based on 2D-FEA at maximum current density condition of $30\text{A}/\text{mm}^2$ and $30\text{A}_{\text{rms}}/\text{mm}^2$ for DC FEC and armature coil, respectively. The average torque obtained is 94.35Nm with the peak-to-peak torque of approximately 215.5Nm, similar peak-to-peak achieves for PM cogging torque. Since in real situation the condition of high cogging torque will results in high vibration and noise. Therefore design improvement should be conducted to reduce the infirmity.

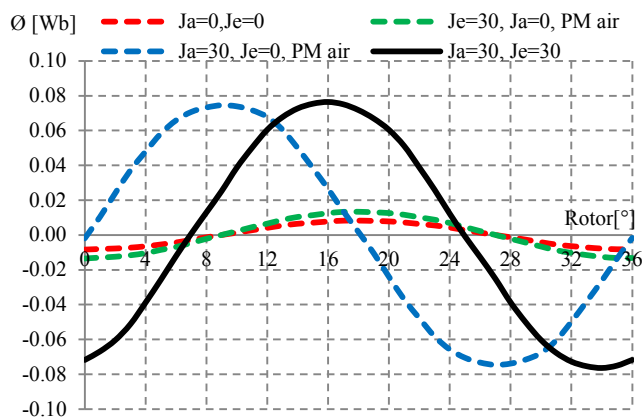


Fig. 9. Flux interaction of PM, DC FEC and armature coil

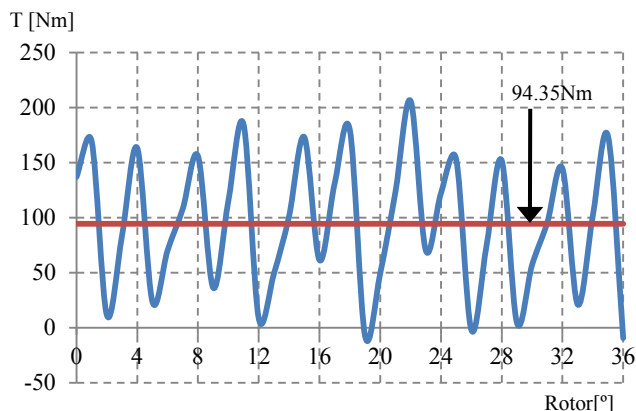


Fig. 10. Instantaneous torque characteristics at maximum DC FEC and armature coil current densities

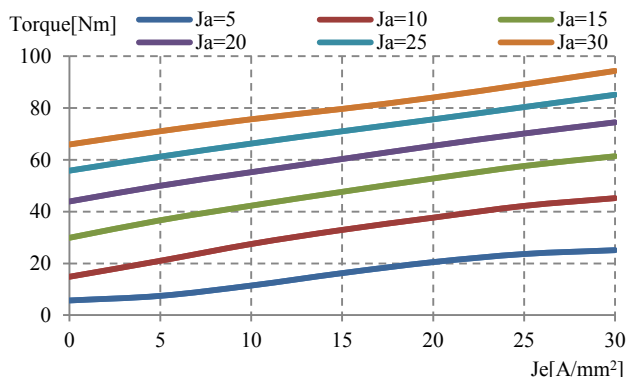


Fig. 11. Comparison of maximum flux linkage of PM with DC FEC and flux from DC FEC only.

C. Torque Characteristics at Various Current Density Conditions

The torque versus DC FEC current density characteristics of the proposed motor is plotted in Fig. 11, where both armature coil and DC FEC current densities are varied from 0 to 30A/mm². According to the conventional theory on d-q coordinate, the torque can be defined as the following fashions under the assumptions that d-axis current is controlled to be zero and voltage drop due to the armature resistance is negligible compared to the induced voltage.

$$T = P_n \cdot (\phi_m + \phi_e) i_q \quad (1)$$

Where P_n is the number of pole-pairs, ϕ_m is the PM flux linkage and ϕ_e is the flux linkage produced by mmf of DC FEC. From the equation it is obvious that the torque generated is proportional to the PM and DC FEC flux. Thus increasing both fluxes will increase the torque.

The plots clearly show that the maximum torque of 94.35Nm is obtained when armature coil and DC FEC current densities are set to the maximum of 30A_{rms}/mm² and 30A/mm², respectively, while the power obtained at the speed of 1200r/min is 11.86kW. The total weight of the proposed motor estimated including rotor core, stator yoke, PMs and coil end of both armature coil and DC FEC is 28.5kg, yield the maximum torque and power density of 3.31Nm/kg and 0.42kW/kg, respectively.

VI. CONCLUSIONS

In this paper, design study and performance analysis of 12-slot/10-pole HEFSM has been investigated. The novelty of the design is the arrangements of DC FEC in radial direction in contrast with traditional HEFSM with the DC FEC arrangements in theta direction. The flux of DC FEC has improved the PM flux of more than four times at maximum DC FEC current density of 30A/mm². A proportional increment on flux generated also gives the advantages of variable flux capabilities. The torque and power achieved are considered acceptable and suitable for various applications. However, design improvement on cogging torque and flux saturation at high current density will be conducted in future.

REFERENCES

- [1] L. Xiaogang, T. A. Lipo, "A synchronous/permanent magnet hybrid AC machine," *IEEE Transactions on Energy Conversion*, vol. 15, no.2 pp. 203–210, June 2000.
- [2] N. Naoe and T. Fukami, "Trial production of a hybrid excitation type synchronous machine," *IEEE International Electric Machines and Drives Conference, (IEMDC 2001)*, pp. 545-547, June 2001.
- [3] D. Fodorean, A. Djerdir, I. A. Viorel, and A. Miraoui, "A double excited synchronous machine for direct drive application-Design and prototype tests," *IEEE Transactions on Energy Conversion*, vol. 22, no. 3 pp. 656–665, Sep. 2007.
- [4] J. A. Tapia, F. Leonardi, T. A. Lipo, "Consequent-pole permanent-magnet machine with extended field-weakening capability," *IEEE Transactions on Industry Applications*, vol. 39, no. 6 pp. 1704-1709, Dec 2003.
- [5] T. Kosaka, N. Matsui, "Hybrid excitation machines with powdered iron core for electrical traction drive applications," *International Conference on Electrical Machines and Systems, (ICEMS 2008)*, pp. 2974 –2979, Oct. 2008.
- [6] T. Kosaka, M. Sridharbabu, M. Yamamoto, and N. Matsui, "Design studies of hybrid excitation motor for main spindle drive in machine tools," *IEEE Transactions on Industrial Electronics*, vol. 57, no.11 pp. 3807–3813, Nov. 2010.
- [7] Z. Chen, Y. Sun, Y. Yan, "Static characteristics of a novel hybrid excitation doubly salient machine," *Proceedings of the Eighth International Conference on Electrical Machines and Systems, (ICEMS 2005)*, vol. 1, pp. 718-721, Sept. 2005.
- [8] K. T. Chau, J. Z. Jiang, W. Yong, "A novel stator doubly fed doubly salient permanent magnet brushless machine," *IEEE Transactions on Magnetics*, vol. 39, no.5 pp. 3001–3003, Sept 2003.

- [9] E. Hoang, M. Lecrivain, and M. Gabsi, "A New Structure of a Switching Flux Synchronous Polyphased Machine with Hybrid Excitation," Proc. of European Conference on Power Electronics and Application, (EPE-2007), Sept 2007.
- [10] M. Kamiya, "Development of Traction Drive Motors for the Toyota Hybrid Systems," *IEEE Transactions on Industrial Application*, Vol.126, No.4, pp.473-479, April 2006.
- [11] Y. Amara, L. Vido, M. Gabsi, E. Hoang, M. Lecrivain, and F. Chabot: "Hybrid Excitation Synchronous Machines: Energy Efficient Solution for Vehicle Propulsion", IEEE Vehicle Power and Propulsion Conference, VPPC 06, pp.1-6, Sept. 2006
- [12] C. Zhao, and Y. Yan: "A review of development of hybrid excitation synchronous machine", Proc. of the IEEE International Symposium on Industrial Electronics, 2005, Vol.2, pp.857-862, June 2005
- [13] R. L. Owen, Z.Q. Zhu, and G.W. Jewell: "Hybrid excited flux-switching permanent magnet machines", Proc. 13th European Conf. on Power Electronics and Applications, EPE 2009, Barcelona, Spain, pp.1-10, 2009
- [14] Yu Wang and Zhiqian Deng: "Comparison of hybrid excitation topologies for flux-switching machines", IEEE Trans. on Magnetics, vol. 48, No. 9, pp. 2518-2527, 2012
- [15] Y. Liao, F. Liang, and T. A. Lipo: "A novel permanent magnet motor with doubly salient structure", in Proc. Conf. Rec. IEEE IAS Annual Meeting, pp. 308-314, Oct. 1992
- [16] K. T. Chau, M. Cheng, and C. C. Chan: "Nonlinear magnetic circuit analysis for a novel stator doubly fed doubly salient machine", IEEE Trans. Magnetics, Vol.38, No.5, pp.2382-2384, Sep. 2002
- [17] W. Hua, M. Cheng, and G. Zhang: "A novel hybrid excitation flux-switching motor for hybrid vehicles", IEEE Trans. Magnetics, Vol.45, No.10, pp.4728-4731, 2009
- [18] E. Hoang, M. Lecrivain, and M. Gabsi: "A new structure of a switching flux synchronous polyphased machine with hybrid excitation", in Proc. Eur. Conf. Power Electron. Appl., pp.1-8, Sep. 2007
- [19] E. Hoang, *et.al.*: "Experimental comparison of lamination material case switching flux synchronous machine with hybrid excitation", Proc. of European Conference on Power Electronics and Applications, No.53, Barcelona, Sept. 2009
- [20] J. T. Chen, Z. Q. Zhu, S. Iwasaki, and R. P. Deodhar: "A Novel Hybrid-Excited Switched-Flux Brushless AC Machine for EV/HEV Applications", IEEE Transactions on Vehicular Technology, Vol.60, No.4, May 2011
- [21] E. Sulaiman, T. Kosaka, and N. Matsui, "Design Improvement and Performance Analysis of 12S-10P Permanent Magnet Flux Switching Machine with Field Excitation Coil" *Journal of Electrical System*, Vol 8, NO. 4, pp. 425-432, Dec 2012.
- [22] E. Sulaiman, T. Kosaka, Y. Tsujimori, and N. Matsui, "Design of 12-Slot 10-Pole Permanent Magnet Flux Switching Machine with Hybrid Excitation for Hybrid Electric Vehicle," Proc. The 5th IET International Conference on Power Electronics, Machine and Drives (PEMD 2010), April 2010.
- [23] E. Sulaiman, T. Kosaka, and N. Matsui, "Design optimization of 12Slot-10Pole hybrid excitation flux switching synchronous machine with 0.4kg permanent magnet for hybrid electric vehicles", Proc. 8th Int. Conference on Power Electronics – ECCE Asia, (ICPE 2011), June 2011.